HHS Public Access

Author manuscript

Science. Author manuscript; available in PMC 2019 July 13.

Published in final edited form as:

Science. 2018 March 30; 359(6383): 1537–1542. doi:10.1126/science.aao0505.

Antibody-mediated inhibition of MICA and MICB shedding promotes NK cell–driven tumor immunity

Lucas Ferrari de Andrade[1,2], **Rong En Tay**[1,2], **Deng Pan**[1,2], **Adrienne M. Luoma**[1,2], **Yoshinaga Ito**[1,2], **Soumya Badrinath**[1,2], **Daphne Tsoucas**[3], **Bettina Franz**[1,2], **Kenneth F. May Jr.**[4], **Christopher J. Harvey**[1], **Sebastian Kobold**[1], **Jason W. Pyrdol**[1], **Charles Yoon**[4,5], **Guo-Cheng Yuan**[3], **F. Stephen Hodi**[4], **Glenn Dranoff**[4,*], and **Kai W. Wucherpfennig**[1,2,†]

[1]Department of Cancer Immunology and Virology, Dana-Farber Cancer Institute, 450 Brookline Avenue, Boston, MA 02215, USA.

[2]Harvard Medical School, 25 Shattuck Street, Boston, MA 02115, USA.

[3]Department of Biostatistics and Computational Biology, Dana-Farber Cancer Institute, 450 Brookline Avenue, Boston, MA 02215, USA.

[4]Department of Medical Oncology, Dana-Farber Cancer Institute, 450 Brookline Avenue, Boston, MA 02215, USA.

[5]Department of Surgery, Brigham and Women's Hospital, 75 Francis Street, Boston, MA 02115, USA.

Abstract

MICA and MICB are expressed by many human cancers as a result of cellular stress, and can tag cells for elimination by cytotoxic lymphocytes through natural killer group 2D (NKG2D) receptor activation. However, tumors evade this immune recognition pathway through proteolytic shedding of MICA and MICB proteins. We rationally designed antibodies targeting the MICA α3 domain, the site of proteolytic shedding, and found that these antibodies prevented loss of cell surface MICA and MICB by human cancer cells. These antibodies inhibited tumor growth in multiple

†**Corresponding author.** kai_wucherpfennig@dfci.harvard.edu.

*Present address: Novartis Institutes for BioMedical Research, 250 Massachusetts Avenue, Cambridge, MA 02139, USA.

Author contributions: K.W.W. and G.D. conceived the study; L.F.d.A., G.D., and K.W.W. designed experimental approaches and interpreted the data; L.F.d.A. characterized antibodies reported in this study and performed therapy as well as mechanistic experiments; R.E.T., Y.I., and L.F.d.A. performed flow cytometry experiments; D.P. analyzed RNA-seq data; S.B. generated some of the recombinant MICA proteins and the B16F10-MICB cell line; A.M.L., D.T., and G.-C.Y. generated single-cell RNA-seq data; B.F. and K.F.M. isolated the first MICA antibody; C.J.H. contributed to early stages of this project; S.K. performed in vivo studies; J.W.P. purified recombinant MICA and MICB proteins; C.Y. provided primary human melanoma cell lines and helped with the design of in vitro functional assays; F.S.H. contributed clinical expertise; and L.F.d.A. and K.W.W. wrote the paper.

Competing interests: The technology has been licensed by the Dana-Farber Cancer Institute to a pharmaceutical company. B.F., K.F.M., C.J.H., J.W.P., F.S.H., G.D., and K.W.W. are inventors on the relevant patent applications (WO 2014144791 A3, WO 2015179627 A1).

Data and materials availability: Materials reported in this study are available through a materials transfer agreement with the Dana-Farber Cancer Institute and by contacting K.W.W. RNA-seq data are deposited in the Gene Expression Omnibus database under accession number GSE109542.

SUPPLEMENTARY MATERIALS

www.sciencemag.org/content/359/6383/1537/suppl/DC1

Materials and Methods

Figs. S1 to S28

References (37–39)

fully immunocompetent mouse models and reduced human melanoma metastases in a humanized mouse model. Antitumor immunity was mediated mainly by natural killer (NK) cells through activation of NKG2D and CD16 Fc receptors. This approach prevents the loss of important immunostimulatory ligands by human cancers and reactivates antitumor immunity.

The stress proteins MICA and MICB are expressed by many human cancers as a consequence of genomic damage, enabling elimination of cancer cells by cytotoxic lymphocytes expressing the natural killer group 2D (NKG2D) receptor (1–6). Engagement of NKG2D receptors triggers natural killer (NK) cell–mediated cytotoxicity and provides a costimulatory signal for CD8 T cells and γδd T cells (7, 8). However, advanced cancers frequently escape this immune mechanism by proteolytic shedding of cell surface–bound MICA and MICB molecules through the coordinated action of a disulfide isomerase (ERp5) and several proteases belonging to the ADAM (a disintegrin and metalloproteinase) and MMP (matrix metalloproteinase) families (9–12). High serum concentrations of shed MICA are associated with disease progression in many human cancers, including melanoma, neuroblastoma, prostate cancer, kidney cancer, multiple myeloma, and chronic lymphocytic leukemia (13–20).

It is impossible to specifically block MICA and MICB shedding in vivo with small-molecule inhibitors because multiple proteases with broad substrate specificities contribute to this process (10–12). The membrane-proximal MICA and MICB α3 domain is the site of proteolytic shedding, whereas the membrane-distal α1 and α2 domains bind to the NKG2D receptor (Fig. 1A) (9, 21, 22). We hypothesized that shedding could be inhibited in a highly specific manner, with antibodies binding to key epitopes on the MICA and MICB α3 domain required for initiation of shedding and that such antibodies would not interfere with NKG2D binding. We further reasoned that the Fc segment of such antibodies could contribute to therapeutic efficacy by engaging activating Fc receptors. We immunized mice with the recombinant MICA α3 domain and identified three monoclonal antibodies (mAbs) (7C6, 6F11, and 1C2) that bound to the α3 domain and the full-length MICA extracellular domain (Fig. 1B and fig. S1, A, B, and D). *MICA* and *MICB* genes are polymorphic, but the α3 domain is more conserved than the α1 and α2 domains, explaining why these antibodies bound to all tested MICA variants and also MICB (fig. S1, B and C).

Functional studies showed that MICA and MICB α3 domain–specific antibodies strongly inhibited MICA shedding by a diverse panel of human tumor cell lines, resulting in a substantial increase in the cell surface density of MICA (Fig. 1, C and D, and fig. S2, A and B). By contrast, the previously reported 6D4 mAb (23) bound outside the MICA α3 domain and did not inhibit MICA shedding (Fig. 1, B to D, and fig. S2B). The α3 domain–specific antibodies also reduced MICA and MICB shedding by murine tumor cell lines expressing cDNAs encoding full-length human MICA or MICB under the control of a lentiviral vector (figs. S2C; S3, A to C; and S4D) but did not affect amounts of secreted MICA by cells expressing only the MICA extracellular domain (fig. S4,C and D). These antibodies minimally affected detection of recombinant soluble MICA by enzyme-linked immunosorbent assay (ELISA) (fig. S4, A and B) and did not interfere with NKG2D binding

to MICA (fig. S5, A to C). Antibody-mediated targeting of the MICA and MICB α3 domain could thus specifically inhibit proteolytic shedding of these NKG2D ligands.

We selected mAb 7C6 for further experiments because it was most effective in stabilizing MICA and MICB on the surface of tumor cells (fig. S3, B and C). NKG2D is an important receptor for NK cell–mediated cytotoxicity, and we found that the 7C6 mAb (with human immunoglobulin G1 Fc region hIgG1) enabled strong NK cell–mediated killing of human tumor cells, including tumor cell lines not targeted by NK cells in the absence of this antibody (Fig. 1E and figs. S6A and S7). Human NK cells also produced higher amounts of interferon-γ (IFN-γ) when cocultured with tumor cells in the presence of the 7C6-hIgG1 mAb (fig. S6B). The 7C6 antibody also inhibited MICA and MICB shedding by short-term human melanoma (24) cell lines generated from meta-static lesions (fig. S8, A to C). These results demonstrate that a MICA α3 domain–specific antibody could enhance the function of human NK cells against tumor cells.

Although only primates have *MICA* and *MICB* genes (1), human MICA is recognized by the murine NKG2D receptor (fig. S9), which enabled preclinical testing in syngeneic, fully immunocompetent mouse tumor models. We introduced the MICA cDNA with a lentiviral vector into murine B16F10 melanoma and CT26 colon cancer cell lines and tested the activity of the 7C6 antibody in lung metastasis models. Treatment with 7C6 antibody (mouse immunoglobulin G2a Fc region, mIgG2a) strongly reduced the number of lung metastases formed by B16F10-MICA tumor cells (Fig. 2, A and B, and fig. S10, A and B). Shed MICA concentrations were high in sera of mice treated with an isotype control antibody but became undetectable in mice treated with 7C6 mAb (Fig. 2C). The 7C6 mAb also demonstrated efficacy in a lung metastasis model with CT26 cells expressing MICA (Fig. 2D) and could be detected on the surface of B16F10-MICA cells in sub-cutaneous tumors (fig. S11, A and B). Also, increased MICA expression was detected on the surface of B16F10-MICA tumor cells when mice were treated with 7C6-mIgG2a compared to isotype control antibody (fig. S11C). Interestingly, endogenous anti-MICA antibodies naturally arose in mice inoculated with MICA-expressing tumor cells (fig. S11D). Murine IgG1 was the predominant isotype for these antibodies (fig. S11E), an isotype associated with poor antitumor activity (25). These endogenous antibodies did not affect detection of recombinant MICA by ELISA (fig. S11F), did not slow tumor growth (fig. S11G), and moderately inhibited detection of shed MICA in serum samples (fig. S11H). Accordingly, 7C6 treatment inhibited growth of subcutaneous B16F10-MICA melanomas more effectively in B cell–deficient mice ($Igh^{-/-}$) that were unable to mount such an antibody response (fig. S11, I and J). The efficacy of the 7C6 mAb was restricted to subcutaneous tumors that expressed full-length MICA or MICB; no therapeutic effect was observed for tumors that secreted the extracellular domain of MICA or that lacked these NKG2D ligands (Fig. 2E). Furthermore, 7C6 mAb inhibited MICA and MICB shedding but did not promote clearance of secreted MICA protein (fig. S12A). These results demonstrate that a mAb that inhibited MICA and MICB shedding had antitumor activity in fully immunocompetent mouse models.

Antibody-mediated depletion revealed that NK cells, but not CD8 T cells, were essential for the therapeutic activity of 7C6 mAb against lung metastases (Fig. 2F and fig. S12B). Furthermore, therapeutic efficacy was lost in perforin (*Prf1*)–but not IFN-g (*Ifng*)–deficient

mice, indicating that NK cell–mediated cytotoxicity represented an essential mechanism (Fig. 2G and fig. S12C). Treatment with 7C6 mAb was associated with tumor cell apoptosis and a substantial reduction of tumor cell load within lung tissue (fig. S13, A to E). The MICA antibody also had activity against established metastases. Treatment was delayed until day 7, when metastases were detectable, and 7C6-mIgG2a reduced serum MICA concentrations and the number of lung metastases while enhancing infiltration of lung tissue by activated NK cells (fig. S14, A to D).

We next examined the changes in gene expression by NK cells induced by MICA antibodies. Human NK cells cocultured with 7C6-hIgG1–pretreated human A375 melanoma cells up-regulated genes associated with NK cell activation and effector functions (fig. S15, A and B). It was previously reported that tumors are infiltrated by group 1 innate lymphoid cells (ILCs), which are composed of NK cells and innate lymphoid cells 1 (ILC1) (26). We sorted group 1 ILCs from meta-static lung tissue by flow cytometry for single-cell RNA sequencing (RNA-seq); these tissue-infiltrating group 1 ILCs expressed CD69, a tissue residency marker, whereas blood group 1 ILCs (likely NK cells) were low in CD69 (fig. S16A). Single-cell RNA-seq demonstrated major differences in the composition and activation state of group 1 ILCs between 7C6-mIgG2a and isotype control treatment groups. In 7C6-mIgG2a–antibody treated mice, most group 1 ILCs (63.2%) were NK cells with a gene expression signature associated with activation and cytotoxicity, including expression of eomesodermin (EOMES), granzyme A (GZMA), granzyme B (GZMB), and perforin 1 (PRF1) (Fig. 3, A and B, and fig. S17, A and B). By notable contrast, a large fraction of cells (49.4%) in isotype control antibody–treated mice were ILC1 with a gene expression signature associated with cytokine and chemokine signaling and inflammation, including expression of the CXCR3 and CXCR6 chemokine receptors and lymphotoxin β (LTB) (Fig. 3, A and B, and fig. S18, A and B) (26). We also identified ILC1 in lung tissue of naïve mice that had not been injected with tumor cells (fig. S19, A and B), indicating that ILC1 originated from a lung-resident cell population. Taken together, these data indicated that treatment with this MICA antibody resulted in a notable activation of tissue-infiltrating NK cells and expression of cytotoxicity genes.

Using flow cytometry, we validated key findings from the single-cell RNA-seq study. Lung-infiltrating NK cells were identified using EOMES and CD49b as markers, whereas lung-resident ILC1 were positive for CD49a, CD226, CXCR3, and CXCR6 (fig. S20A). Staining for GZMA allowed identification of activated NK cells that also expressed EOMES and CD49b (fig. S20A). Quantification of $EOMES^+$ $GZMA^+$ cells demonstrated an approximately fourfold increase of these activated NK cells (adjusted for tumor burden) on days 4, 7, and 11 in 7C6-mIgG2a–treated mice compared to isotype control antibody–treated mice with lung metastases (Fig. 3C and fig. S20C). Also, the presence of lung metastases increased absolute numbers of lung-resident NK cells and ILC1 as shown by comparison of naïve mice and isotype control antibody–treated mice with lung metastases (figs. S16B and S20B). ILC1 expressed higher amounts of NKG2D at the protein level, but not at the mRNA level, compared to NK cells (Fig. 3B and fig. S20A). Also, surface levels of NKG2D were higher among tissue-infiltrating NK cells than blood NK cells (figs. S16C and S21A). However, NKG2D surface levels were substantially reduced among tissue-resident NK cells and ILC1 in tumor-bearing mice compared to naïve mice, even when tumor cells did not

express MICA (figs. S21, A and B, and S16C), suggesting that signals from the tumor microenvironment (such as transforming growth factor–β) contributed to lower NKG2D levels within metastases (27, 28).

NK cells are regulated by multiple activating and inhibitory receptors, and both NKG2D and CD16 Fc receptors strongly modulate NK cell functions (29). We introduced two mutations into the 7C6-hIgG1 and mIgG2b heavy chains [aspartate to alanine at position 265 (D265A) and asparagine to alanine at position 297 (N297A), or DANA] to abrogate binding to activating Fc receptors (25). 7C6-DANA mutant antibodies did not bind to the activating Fc receptor expressed by NK cells (CD16a) but retained MICA binding (fig. S22, A to D). The 7C6-mIgG2b-DANA mutant antibody inhibited MICA shedding to the same extent as nonmutated mIgG2b and mIgG2a forms (fig. S23, A and B). Pretreatment of A375 cells with the 7C6-hIgG1-DANA mutant mAb induced killing by human NK cells, and this effect was blocked with an NKG2D-blocking mAb. This result demonstrates that inhibition of MICA shedding could induce NK cell–mediated cytotoxicity in the absence of Fc receptor engagement (Fig. 3D and fig. S23C). The 7C6-DANA mutant antibody also had therapeutic activity in the B16F10-MICA lung metastasis model, and therapeutic benefit was lost when a NKG2D-blocking antibody was administered (fig. S23, D and E). These results demonstrate that inhibition of MICA and MICB shedding by 7C6 restored NKG2D-mediated tumor immunity.

Engagement of multiple activating receptors enhances NK cell effector functions (29, 30). 7C6 mAb with a fully functional Fc region (hIgG1) triggered stronger cytotoxicity by human NK cells than the 7C6-hIgG1-DANA mutant (Fig. 3D). We also addressed the contribution of NKG2D and CD16 Fc receptors to NK cell functions in vivo by transfer of wild-type (WT) or mutant NK cells into *Rag2*$^{-/-}$ *Il2rg*$^{-/-}$ mice that were T cell and NK cell deficient. The most consistent reduction in the number of lung metastases was observed after transfer of WT NK cells. The therapeutic effect was maintained (but more variable) after transfer of NK cells deficient in either NKG2D (*Klrk1*$^{-/-}$) or CD16 (*Fcgr3a*$^{-/-}$). By notable contrast, antibody treatment was ineffective after transfer of NK cells that lacked both NKG2D and CD16 receptors, although shed MICA was still reduced (Fig. 3E and fig. S12D). NKG2D and CD16 Fc receptors were also both required for optimal inhibition of subcutaneous tumor growth (fig. S24, A and B). These data demonstrate that 7C6 mAb activated NK cells through two important receptors, the NKG2D and CD16 Fc receptors.

In the syngeneic tumor models described above, *MICA* and *MICB* gene expression was induced by a heterologous promoter. However, in human cancers, *MICA* and *MICB* gene expression is endogenously activated in response to malignant transformation (1). To test this therapeutic concept with human cancer cells and NK cells, NOD-*scid*IL2Rg^{null} (NSG) mice were reconstituted with human NK cells, followed by injection of human A2058 melanoma cells (Fig. 4A). IL-2 was injected every other day for a week to support NK cell survival. Inoculation of A2058 cells by an intravenous route resulted not only in lung metastases but, surprisingly, also widespread metastases in many other organs (fig.S25C). Significantly fewer lung metastases were present in mice reconstituted with human NK cells and treated with 7C6-hIgG1 mAb (Fig. 4B and fig. S25A). Antibody treatment also reduced the spread of metastases to many other organs (fig. S25, C to E). Metastases were

particularly prominent in the liver and caused liver damage, as measured by a serum biomarker (alanine transaminase activity). Interestingly, 7C6-hIgG1 treatment substantially reduced the number of liver metastases and prevented liver damage even without NK cell transfer (Fig. 4C and fig. S26A). Liver-resident F4/80^{high} macrophages (Kupffer cells) that expressed activating Fc receptors (fig. S26B) had higher surface levels of the CD80 activation marker in 7C6-hIgG1 treated mice (fig. S26C). Macrophage depletion with clodronate liposomes abrogated the therapeutic activity of 7C6-hIgG1 antibody against liver metastases (Fig. 4D) but had no negative effect on therapeutic efficacy in the lung metastasis model in immunocompetent mice (fig. S27). Human macrophages cultured in vitro express MICA and MICB, and treatment with acetylated low-density lipoproteins, a model of foam cells present in atherosclerotic lesions, increased MICA and MICB expression (31). Treatment with 7C6-hIgG1 antibody inhibited MICA shedding and increased MICA and MICB surface levels on macrophages (fig. S28, A to C). These mechanisms account for the significant survival benefit of 7C6-hIgG1 treatment in this humanized metastasis model (Fig. 4E). These data demonstrate the therapeutic activity of a MICA α3 domain–specific antibody in a humanized metastasis model by activating NK cells and macrophages in an organ-dependent manner.

We found that MICA and MICB α3 domain–specific antibodies substantially increased the density of the stimulatory MICA and MICB ligands on the surface of tumor cells, reduced shed MICA amounts, and induced NK cell–mediated tumor immunity. This therapeutic strategy restores the function of an activating immune pathway that promotes clearance of stressed and transformed cells (Fig. 4F). We propose that the association between MICA and MICB shedding and cancer progression is primarily due to the loss of immunostimulatory NKG2D ligands on the tumor cell surface, although shed MICA may also be a relevant contributing factor. Interestingly, sheddingofthehigh-affinitymurineMULT-1ligand of NKG2D enhances antitumor immunity by inhibiting chronic NKG2D engagement of intratumoral NK cells by myeloid cells that express RAE-1, a murine NKG2D ligand (32). Soluble MICA and MICB have a substantially lower affinity for the NKG2D receptor than MULT-1, which may explain why shed MICA and MICB do not have such a stimulatory function (1). Given that MICA and MICB are widely expressed in human cancers, MICA and MICB antibodies may hold promise for both solid and hematological malignancies (14, 33–36). Such antibodies could be used in combination with established therapies that induce or enhance MICA and MICB expression through genomic damage pathways, including local radiation therapy or antibody-drug conjugates that deliver toxic payloads to tumor cells (4). MICA antibodies are also of considerable interest as a combination partner with other immunotherapies to activate NK cells and enhance cytotoxic T cell function for protective antitumor immunity.

Supplementary Material

Refer to Web version on PubMed Central for supplementary material.

ACKNOWLEDGMENTS

We thank H.-J. Kim for providing Rag2$^{-/-}$ gc$^{-/-}$ mice, C. Sharma for providing the HEPG2 and MDA-MB-231 cell lines, and M. J. Smyth for providing the RMA-S parental cell line. We thank D. Neuberg for advice regarding statistical analyses.

Funding: L.F.d.A. was supported by a Friends for Life Neuroblastoma Fellowship; D.P. is a Cancer Research Institute–Robertson Foundation Fellow; R.E.T. was supported by an Agency for Science, Technology, and Research (A*STAR) Graduate Fellowship; A.M.L. was supported by a Cancer Immunology Training Grant (T32 CA207021); S.B. was supported by a U.S. Department of Defense fellowship (DOD CA150776); K.F.M. was supported by an American Society of Clinical Oncology Young Investigator Award, a Prostate Cancer Foundation Young Investigator Award, and a National Cancer Institute (NCI) T32 grant; K.W.W. was supported by a grant from NCI (R01 CA173750); and K.W.W. and G.D. were supported by a grant from the Melanoma Research Alliance.

REFERENCES AND NOTES

1. Raulet DH, Gasser S, Gowen BG, Deng W, Jung H, Annu. Rev. Immunol 31, 413–441 (2013). [PubMed: 23298206]
2. Vantourout P et al., Sci. Transl. Med 6, 231ra49 (2014)
3. Bahram S, Bresnahan M, Geraghty DE, Spies T, Proc. Natl. Acad. Sci. U.S.A 91, 6259–6263 (1994) [PubMed: 8022771]
4. Gasser S, Orsulic S, Brown EJ, Raulet DH, Nature 436, 1186–1190 (2005). [PubMed: 15995699]
5. Lanier LL, Cancer Immunol. Res 3, 575–582 (2015). [PubMed: 26041808]
6. Hayakawa Y et al., J. Immunol 169, 5377–5381 (2002). [PubMed: 12421908]
7. Bauer S et al., Science 285, 727–729 (1999). [PubMed: 10426993]
8. Groh V et al., Nat. Immunol 2, 255–260 (2001). [PubMed: 11224526]
9. Kaiser BK et al., Nature 447, 482–486 (2007). [PubMed: 17495932]
10. Boutet P et al., J. Immunol 182, 49–53 (2009). [PubMed: 19109134]
11. Groh V, Wu J, Yee C, Spies T, Nature 419, 734–738 (2002). [PubMed: 12384702]
12. Waldhauer I et al., Cancer Res 68, 6368–6376 (2008). [PubMed: 18676862]
13. Raffaghello L et al., Neoplasia 6, 558–568 (2004). [PubMed: 15548365]
14. Jinushi M et al., Proc. Natl. Acad. Sci. U.S.A 105, 1285–1290 (2008). [PubMed: 18202175]
15. Holdenrieder S et al., Int. J. Cancer 118, 684–687 (2006). [PubMed: 16094621]
16. Koguchi Y et al., Cancer Res 75, 5084–5092 (2015). [PubMed: 26627641]
17. Wu JD et al., J. Clin. Invest 114, 560–568 (2004). [PubMed: 15314693]
18. Chitadze G et al., Int. J. Cancer 133, 1557–1566 (2013). [PubMed: 23526433]
19. Yang FQ et al., Actas Urol. Esp 38, 172–178 (2014). [PubMed: 24461475]
20. Huergo-Zapico L et al., Cancer Immunol. Immunother 61, 1201–1210 (2012). [PubMed: 22215138]
21. Wang X et al., Biochem. Biophys. Res. Commun 387, 476–481 (2009). [PubMed: 19615970]
22. Li P et al., Nat. Immunol 2, 443–451 (2001). [PubMed: 11323699]
23. Groh V, Steinle A, Bauer S, Spies T, Science 279, 1737–1740 (1998). [PubMed: 9497295]
24. Izar B et al., Pigment Cell Melanoma Res 29, 656–668 (2016). [PubMed: 27482935]
25. Nimmerjahn F, Ravetch JV, Science 310, 1510–1512 (2005). [PubMed: 16322460]
26. Gao Y et al., Nat. Immunol 18, 1004–1015 (2017). [PubMed: 28759001]
27. Lee J-C, Lee K-M, Kim D-W, Heo DS, J. Immunol 172, 7335–7340 (2004). [PubMed: 15187109]
28. Clayton A et al., J. Immunol 180, 7249–7258 (2008). [PubMed: 18490724]
29. Long EO, Kim HS, Liu D, Peterson ME, Rajagopalan S, Annu. Rev. Immunol 31, 227–258 (2013). [PubMed: 23516982]
30. Bryceson YT, March ME, Ljunggren H-G, Long EO, Blood 107, 159–166 (2006). [PubMed: 16150947]
31. Ikeshita S, Miyatake Y, Otsuka N, Kasahara M, Exp. Mol. Pathol 97, 171–175 (2014). [PubMed: 24997223]

32. Deng W et al., Science 348, 136–139 (2015). [PubMed: 25745066]
33. Zhang J, Basher F, Wu JD, Front. Immunol 6, 97 (2015). [PubMed: 25788898]
34. Vetter CS et al., J. Invest. Dermatol 118, 600–605 (2002). [PubMed: 11918705]
35. Pende D et al., Cancer Res 62, 6178–6186 (2002). [PubMed: 12414645]
36. Liu G et al., J. Clin. Invest 123, 4410–4422 (2013). [PubMed: 24018560]

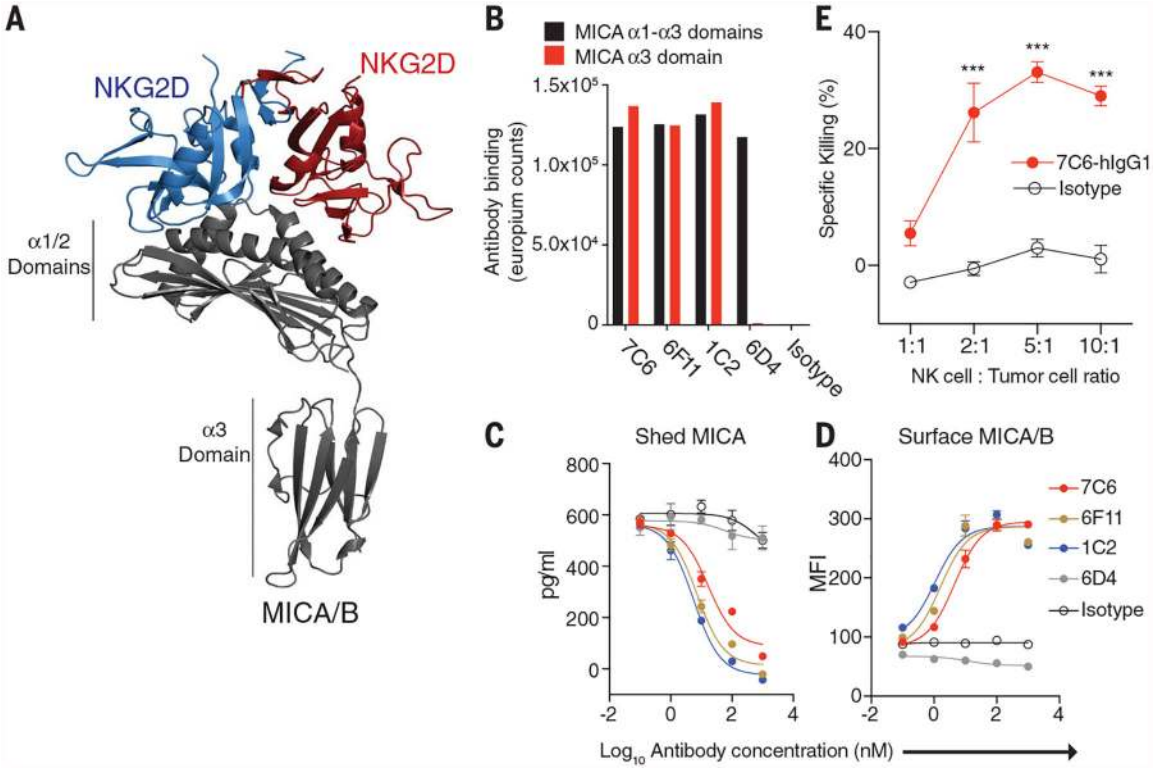

Fig. 1. MICA and MICB α3 domain–specific antibodies inhibit shedding and stabilize the protein on the surface of human tumor cells for recognition by NK cells.

(**A**) Illustration of MICA protein bound to a NKG2D homodimer (Protein Data Bank 1HYR). MICA is colored in grayand the NKG2D homodimer in blue and red. The NKG2D dimer binds to the α1 and α2 domains;the α3 domain is the site of proteolytic cleavage. (**B**) Binding of mAbs to immobilized MICA α3 domain or MICA α1 to α3 domains detected with a fluorescence-based ELISA (one representative of three independent experiments). (**C** and **D**) A375 cells were treated for 24 hours with the indicated mAbs. (C) MICA α3 domain–specific mAbs (7C6, 6F11, 1C2) inhibit MICA release into the supernatant, as quantified by sandwich ELISA; mAb 6D4 binds outside the MICA α3 domainand thus does not inhibit shedding. Data show mean ± SD for triplicate measurements from one representative of three independent experiments. (D) MICA α3 domain–specific mAbs stabilize MICA surface expression, as determined by flow cytometry using phycoerythrin (PE)–labeled 6D4 mAb. MFI, mean fluorescence intensity. Data show mean ± SD for triplicate measurements from one representative of three independent experiments. (**E**) Human NK cells exhibit cytotoxicity against A375 cells in the presence of 7C6-hIgG1 antibody (66.7 nM) but not isotype control antibody. Mean ± SD for quadruplicate measurements. ***$P < 0.001$ calculated by two-way analysis of variance (ANOVA) and Bonferroni's post hoc test. Representative of three independent experiments (each experiment was done with different human NK cell donors).

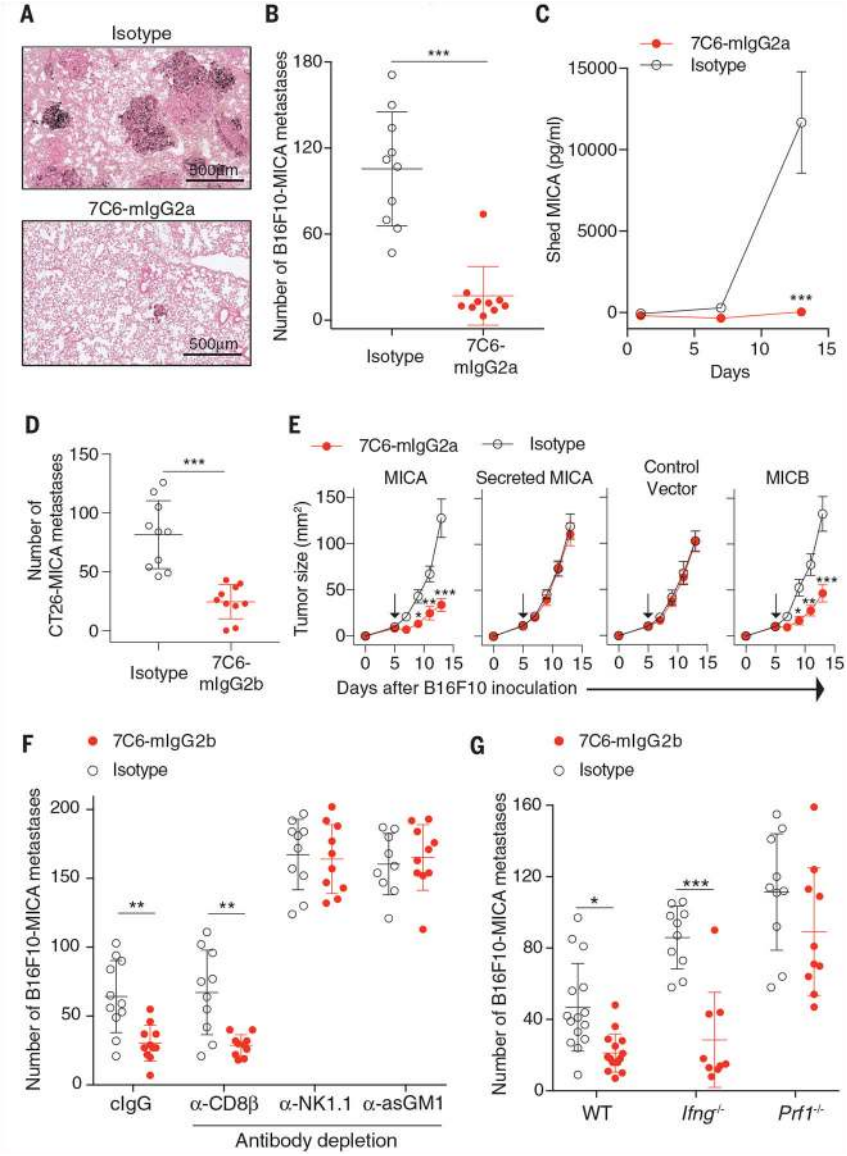

Fig. 2. Antitumor activity of antibodiesthat inhibit MICA and MICB shedding.

(**A** to **C**) C57BL/6 mice were injected intravenously with B16F10-MICA cells and treated with 7C6-mIgG2a, 7C6-mIgG2b, or isotype control antibodies (200 μg per injection) on days 1, 2,7, and 10. (A) Histological analysis (Fontana-Masson staining) of lung tissue demonstrated an apparent reduction in the number and size of metastases in mice that were treated with the MICA antibody (representative of five mice). (B) MICA antibody treatment reduced the number of superficial lung metastases counted by stereomicroscopy on day 14. Data indicate mean ± SD of pooled data from two independent experiments. (C) Serum concentrations ofshed MICA. Data show mean ± SEM for five mice per group and one representative of two independent experiments. (**D**) 7C6-mIgG2b antibody had activity against CT26-MICA lung metastases (intravenous injection of tumor cells into Balb/c mice; antibody injection on days 1, 2, 7, and 14; lung metastases counted on day 21). Data indicate mean ± SD of pooled data from two independent experiments. (**E**) Analysis of therapeutic

activity of 7C6-mIgG2a antibody against subcutaneous B16F10 tumors that expressed full-length MICA or MICB or a secreted form of MICA, or were transduced with control vector. Tumor cells were inoculated into *Igh*$^{-/-}$ mice; treatment with 7C6-mIgG2a or isotype control antibodies was started on day 5 (arrows) and repeated at every tumor measurement. Data show mean ± SEM for10 mice per group pooled from two independent experiments. (**F** and **G**) Efficacy of 7C6 antibody treatment required NK cells and their cytotoxic function. Same experimental design as in (A) to (C). (F) Quantification of pulmonary metastases in mice that were CD8 Tcell depleted (α-CD8β) or NK cell depleted (α-NK1.1 and a-asGM1). Data indicate mean ± SD pooled from two independent experiments. (G) Mice deficient for PRF1-mediated cytotoxicity, but not IFN-γ production, were unresponsive to 7C6 mAb treatment. Data indicate mean ± SD pooled from two independent experiments. *$P < 0.05$, **$P < 0.01$, and ***$P < 0.001$, calculated by unpaired Student's t test (B) and (D) and two-way ANOVA and Bonferroni's post hoc test (C) and (E) to (G).

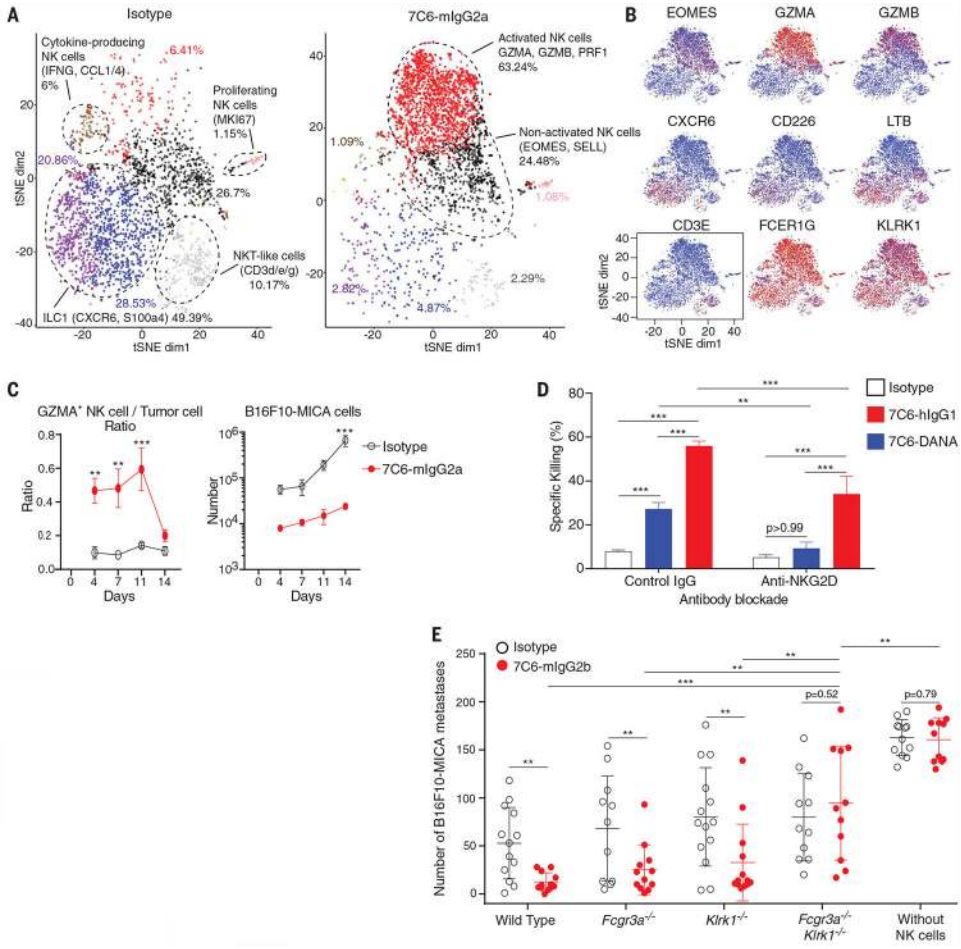

Fig. 3. NK cell activation by dual NKG2D receptor and CD16 engagement enhances antitumor immunity.

(**A** and **B**) Single-cell RNA-seq analysis of lung-infiltrating group 1 ILCs. On day 7 after intravenous injection of B16F10-MICA tumor cells, lung-infiltrating group 1 ILCs were isolated on the basis of NK1.1 and NKp46 staining (cells pooled from nine mice for isotype control and eight mice for 7C6-mIgG2a groups). Natural killer T–like cells that expressed both T cell and NK cell markers were also identified (even though TCRβ and CD3ε positive cells had been excluded), likely because the T cell receptor (TCR) is internalized after T cell activation.(A) t-distributed stochastic neighbor embedding (tSNE) plots illustrating identified cell populations in isotype control (left)–and 7C6-mIgG2a (right)–treated mice. Major populations and key markers are indicated. (B) Expression of key genes in group 1 ILCs on pooled data from isotype- and 7C6-mIgG2a–treated groups. FCER1G, Fc epsilon receptor gamma chain. (**C**) Fluorescence-activated cell sorting analysis of lung-infiltrating activated NK cells (EOMES^{+} GZMA^{+}) across indicated time points relative to tumor burden (five mice per group and time point). Data indicate mean ± SEM; days 7 and 14 are representative of two independent experiments. (**D**) Contribution of NKG2D and Fc receptor activation to NK cell–mediated cytotoxicity. A375 cells were treated for 48 hours with indicated antibodies and then cocultured for 4 hours with human NK cells in a ^{51}Cr-release assay. The 7C6-hIgG1-DANA mutant lacked binding to activating Fc receptors. NKG2D

recognition was blocked with anti-NKG2D mAb 1D11. Data indicate mean ± SD and one representative of three independent experiments. (**E**) Both NKG2D and CD16 receptors contribute to therapeutic activity of MICA antibody. *Rag2*$^{-/-}$ *Il2rg*$^{-/-}$ mice were reconstituted with WT NK cells or NK cells mutant for NKG2D (*Klrk1*) and/or CD16 (*Fcgr3a*) genes. Mice werethen injected intravenously with B16F10-MICA cells and treated with 7C6-mIgG2b or isotype control antibodies, and lung metastases were quantified on day 14. Data indicate mean ± SD of pooled data from three independent experiments. $^{**}P < 0.01$ and $^{***}P < 0.001$, calculated by two-way ANOVA with Bonferroni's post hoc test (C) and (D) or multiple two-tailed unpaired Student's *t* test (E).

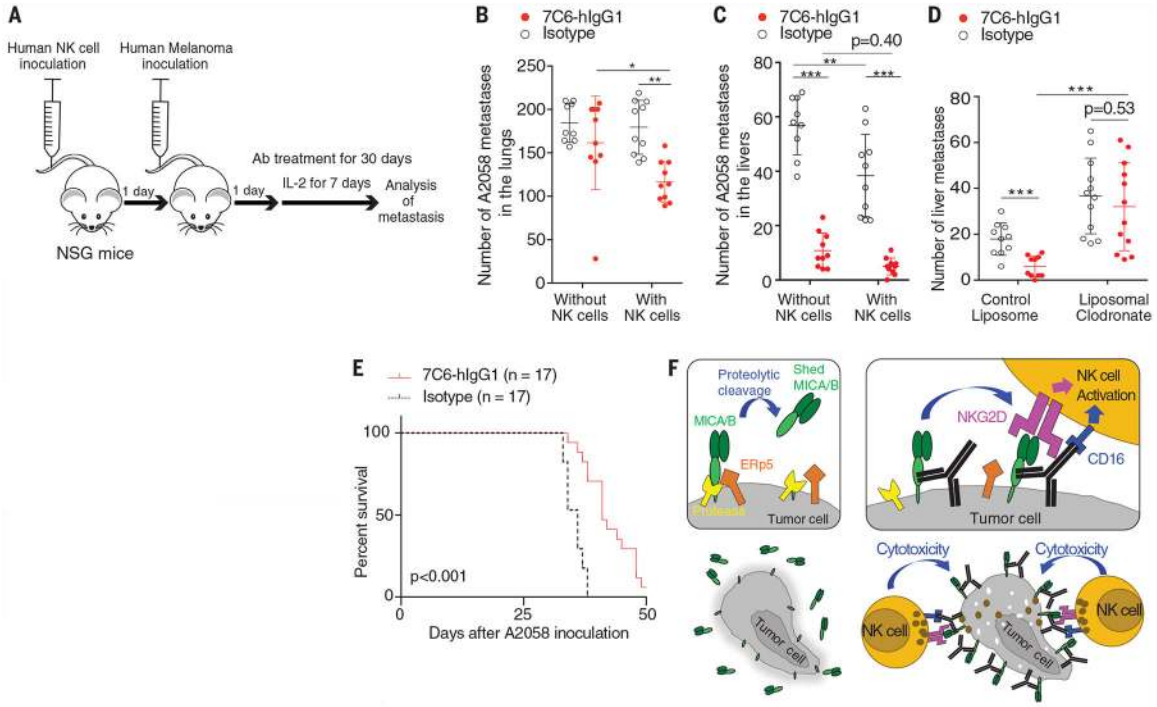

Fig. 4. MICA antibody shows therapeutic activity in a metastasis model with human tumor cells and human NK cells.

(**A** to **C**) NSG mice were reconstituted with IL-2 pretreated human NK cells. NK cell survival was supported by injection of human IL-2 on alternate days until day 8. One day after NK cell transfer, A2058 cells were injected intravenously into all mice. 7C6-hIgG1 or isotype control antibodies were administered on days1 and 2 after tumor inoculation and then once per week. On day 30, mice were euthanized, and metastases were counted in different organs. (A) Outline of the experimental procedure. (B) Quantification of the number of lung metastases by stereomicroscopy. Data are mean ± SD of pooled data from two independent experiments. (C) Quantification of liver metastases by stereomicroscopy. Data are mean ± SD of pooled data from two independent experiments. (**D**) Liposomal clodronate (or control liposomes) were injected intravenously to deplete liver macrophages (same day as tumor cell inoculation and then once per week). Liver metastases were quantified by stereomicroscopy3 weeks after tumor inoculation. Tumor cell inoculation and antibody treatments were done as shown in (A) but without NK cell reconstitution and with analysis of metastases a week earlier. Data are mean ± SD of pooled data from two independent experiments. (**E**) Survival analysis of mice reconstituted with human NK cells, inoculated intravenously with human melanoma cells, and treated with isotype or 7C6-hIgG1 antibodies. Same conditions as in (A). Data are pooled from two independent experiments.(**F**) Cartoon illustrating proposed therapeutic mechanism. $*P < 0.05$,$**P < 0.01$, and $***P < 0.001$, calculated by two-way ANOVA with Bonferroni's post hoc test (B) and (C) or multiple two-tailed unpaired Student's *t* test(D). In (E), the comparison of survival curves is by Mantel-Cox test.